

Ab-initio molecular orbital theory of hydrogenation of LiAl and Li₂Al₂: The magic clusters (LiAlH₄) and (LiAlH₄)₂

Sandeep Nigam, Chiranjib Majumder,* and S. K. Kulshreshtha
Chemistry Division, Bhabha Atomic Research Centre, Mumbai 400085, India

(Received 18 June 2005; revised manuscript received 18 January 2006; published 24 March 2006)

Interaction of hydrogen atoms with light metal alloy clusters such as LiAl and Li₂Al₂ have been investigated under the linear combination of atomic and molecular orbital approach using the post-Hartree-Fock and density functional formalism under the Perdew-Burke-Erzerhof and Lee-Yang-Parr exchange correlation functional. A correlation consistent polar valence triple zeta basis set was employed for this purpose. The saturation composition for Li:Al:H is found to be 1:1:4, reflecting the bulk stoichiometry even in the smallest cluster. The sequential attachment of H atoms to the Li₂Al₂ cluster shows that for $n > 6$, the Al-Al bond in the Li₂Al₂H_{*n*} cluster dissociates and tetrahedral (AlH₄)^{δ-} moiety is formed. Other than inertness towards further reaction, the Li₂Al₂H₈ cluster thus formed shows higher binding energy, ionization potential and low electron affinity, characteristics of a highly stable species. Based on the energetics it is found that the dimerization energy of LiAlH₄ is 1.85 eV, which is significantly higher than the interaction energy usually observed for molecules or stable clusters. The higher binding energy of the (LiAlH₄)₂ has been attributed to the increased coordination of Li, where additional bonds are formed between Li^{δ+} and H^{δ-} by the electrostatic force of attraction.

DOI: [10.1103/PhysRevB.73.115424](https://doi.org/10.1103/PhysRevB.73.115424)

PACS number(s): 73.22.-f, 36.40.Cg, 36.40.Ei, 36.40.Qv

I. INTRODUCTION

One of the most interesting aspects of cluster science is the nonmonotonous variation of their physicochemical properties as a function of size.¹ This is essentially due to the discrete nature of the electronic energy levels of such finite size systems, which eventually form the band structure for bulk systems and show material specific properties. For a number of systems the existence of magic clusters, which show extra stability as to their nearest neighbors reflected by their larger ion signal intensity in the mass spectra. Fundamental understanding of the electronic and geometric structure is essential to shed light of their physicochemical properties at the atomic scale. Based on a large number of studies² it has been realized that the stability of metal clusters is governed either by their electronic or the atomic structures. For small alkali metal clusters which follow electronic structure model shows magic behavior for clusters having 8, 20, 40, ..., number of atoms.³ On the other hand for covalent clusters where directional bonding governs the stability follows atomic structure to decide the relative stabilities.⁴ The stability of magic clusters thus synthesized is characterized by their large binding energy, high ionization potential, low electron affinity, and low reactivity, etc. Therefore, it is expected that two magic cluster will interact weakly through van der Waals interaction mechanism. The low interaction energies of two magic clusters such as Mg₄ or Na₈ which was found to be 0.8 and 0.36, respectively, corroborate this effect.^{5,6} At this point it is worth mentioning that molecules, which are formed by few atoms, bear all signatures of a magic cluster in their own right are slightly different due to their fixed stoichiometry and higher stability. Therefore, any molecule can be considered as magic cluster but opposite is not true. Fullerenes are well known examples of both magic clusters and molecules. Due to the larger stability of molecules the interaction between them should be even weaker

than that observed for magic clusters. To illustrate this effect we can take the example of interaction between two methane molecules which shows an interaction energy of 0.02 eV.⁷ Unlike this, the interaction between two metal hydrides was found to be different. In a previous study Rao *et al.* have shown that although AlH₃ is a magic cluster but two AlH₃ bind with a release of 1.54 eV energy.⁸

Light metal alloys have been projected as the most potential hydrogen storage materials because of very high hydrogen contents in its hydride.⁹ Nanostructured materials having larger surface area show higher reactivity as compared to their bulk counterparts. Theoretical studies are available on the hydrogenation of light metal clusters, where the interaction between metal and hydrogen atoms was found to govern either by ionic or covalent bonds.¹⁰ However, to the best of our knowledge no reports are available on the interaction of hydrogen with metal alloy clusters. The objective of the present study is to investigate the interaction of hydrogen with light metal alloy clusters at the atomic scale. In this work we have investigated the hydrogenation behavior of LiAl and Li₂Al₂ clusters using the *ab initio* molecular orbital theory. In particular, we have emphasized the hydrogen uptake behavior of these clusters to verify if the hydrogen content of LiAl clusters could be enhanced at the atomic scale. The results reveal that even at the smallest scale the saturation composition remained as 1:1:4 for Li, Al, and H, respectively, reflecting the bulk stoichiometry. Another important aspect, which deals with the interaction of magic clusters, which are considered as building blocks to form bulk solid, has been demonstrated with unusual behavior. We have discussed in the previous section that due to high stability, magic clusters or molecules interact weakly through van der Waals force which can be illustrated from the low binding energy of dimer formation, ranging from 0.02 to 0.5 eV. In sharp contrast to this, we have estimated significantly high interaction energy between two molecules of LiAlH₄, which

is also a magic cluster by its own right. Details of the ground-state geometries and energetics of LiAlH_n ($n=1-4$) and $\text{Li}_2\text{Al}_2\text{H}_n$ ($n=1-8$) clusters along with the methodology employed to calculate these parameters, are presented in the following sections

II. COMPUTATIONAL DETAILS

The *ab initio* molecular orbital theory methods, as implemented in the GAMESS software, were used to optimize the geometry of several possible isomeric structures of these clusters.¹¹ From the literature¹² it is known that in some cases DFT based calculations can show better results than MP2 level of theory. However, the accuracy can vary depending on the exchange correlation functional chosen for the specific system. In order to obtain accurate description of the interaction between different elements test calculations were carried out for all the homoatomic and heteroatomic dimers under both density functional theory¹³ (DFT) and a post Hartree-Fock method such as Møller-Plesset perturbation theory incorporating the energy correlation effects truncated at second-order¹⁴ (MP2) with extended basis sets such as 6-31G(*d,p*),¹⁵ 6-311++G(*d,p*),¹⁵ and correlation consistent (cc) polar valence triple zeta (pVTZ).¹⁵ The results are summarized in Table I. From Table I, it is seen that under DFT, Perdew-Burke-Erzerhof (PBE) and Lee-Yang-Parr (LYP) exchange correlation functional¹⁷ shows good agreement with experimental values. Further, it has been noticed that although MP2/6-31G(*d,p*) shows good agreement in terms of the bond lengths but the binding energies are underestimated. However, with the increase in the basis functions the results improve consistently. A comparison of bond lengths and binding energy for all dimers (Table I) suggest that, while DFT shows better agreement for Li-Li, Al-Al, and Li-H, interactions of Al-H, H-H, and Al-Li are better under the MP2/cc-pVTZ level in comparison to that of experimental results. Based on this criteria, we have employed MP2/6-31G(*d,p*) method for the optimization of several isomeric structures of $\text{Li}_2\text{Al}_2\text{H}_n$ clusters followed by single point total energy calculation of the lowest energy isomers using the MP2/cc-pVTZ level of calculation. In order to compare the results obtained from the MP2 method, all calculations were repeated under the DFT formalism using the PBE-LYP/cc-pVTZ level of theory. The agreement between these two models was found to be good. The spin polarized calculations were performed considering both singlet and triplet spin state for even number of hydrogen atom and doublet for odd number of hydrogen atom being attached to these metal clusters.

III. RESULTS

The ground-state geometries of LiAlH_n clusters are shown in Fig. 1. It was found that the H atom prefers to bind with Al atom than Li. This can be attributed to the higher Al-H bond energy than Li-H as predicted in Table I. In Table II, we have summarized the inter-atomic separations between Al-H, Li-H, and Al-Li. It is clear that the interatomic separation between Al-Li decreases with increase in H content

and finally it saturates at four. For LiAlH_4 cluster, four hydrogen atoms surround the Al with tetrahedral arrangement. We note that unlike in case of AlH_4 , where molecular hydrogen adsorption was found,⁸ for LiAlH_4 all four hydrogen atoms adsorbed on LiAl dimer dissociatively. This is further clear from the highest H atom attachment energy as shown in Fig. 2. The point charge distribution estimated based on Mulliken population analysis shows that while Al and Li acts as donor by transferring 0.73 and 0.58 electronic charges, respectively, H atoms act as acceptor with an average of 0.32 electronic charges.

For Li_2Al_2 cluster, the lowest energy isomer shows rhombus structure with D_{2h} symmetry (Al and Li atoms occupying the opposite corners). The interatomic separation between Li and Al atom is 2.71 Å and the angle between Al-Li-Al is 52.7° and Li-Al-Li is 127.3°. The *cis*-isomer is found to be 0.93 eV higher in energy as compared to the *trans*-isomer. The charge distribution analysis of the Li_2Al_2 cluster suggests that each Li atom donates 0.36 electronic charge towards Al which is consistent with the higher electropositive character of Li as compared to Al. The Al-Al separation is found to be 2.41 Å which is shorter by 0.07 Å as compared to that of dimer. The average binding energy of Li_2Al_2 cluster is found to be 1.19 eV/atom. In the following section we will describe the hydrogenation behavior of Li_2Al_2 cluster.

The H uptake behavior of Li_2Al_2 cluster has been studied through sequential interactions of H atoms. In Fig. 3 we have depicted some low-lying isomers of $\text{Li}_2\text{Al}_2\text{H}_n$ clusters. The bond length, binding energy/atom, H-uptake energy and Mulliken point charge distribution of $\text{Li}_2\text{Al}_2\text{H}_n$ clusters obtained are listed in Table III. It is found that on hydrogen uptake by Li_2Al_2 cluster, the Al-Al bond gets weaker and finally it ruptures for $n > 6$ and $(\text{AlH}_4)^{\delta-}$ moiety is formed with tetrahedral configuration of H atoms surrounding the Al atom. The details of the geometries have been given below.

A. H uptake on the Li_2Al_2 cluster

Li₂Al₂H and Li₂Al₂H₂. The adsorption of H on the Li_2Al_2 cluster has been studied through sequential interactions of H atom i.e., first the geometry of the $\text{Li}_2\text{Al}_2\text{-H}$ has been optimized by placing the H atom at all possible sites of Li_2Al_2 cluster. Then the second H atom is interacted with $\text{Li}_2\text{Al}_2\text{-H}$ cluster and the ground-state geometry was found by taking all possible configurations for geometry optimization. The H atom binds at the bridge position along the Al-Al bond. This leads to elongation of the Al-Al bond as the additional charge localized along Al-Al bond in the free Li_2Al_2 cluster is transferred to the H atom. Some of the higher energy isomers for $\text{Al}_2\text{Li}_2\text{H}$ and $\text{Al}_2\text{Li}_2\text{H}_2$ are shown in Fig. 3(a)–3(g). From this figure it is clear that H prefers to bind with Al atom. The ground state geometry shows that $\text{Li}_2\text{Al}_2\text{H}_2$ cluster has a bent rhombus skeleton of Li_2Al_2 where the two hydrogen atoms are attached to the two Al atoms at the opposite orientation in such a way that inside hydrogen atom binds to both of the lithium atoms while other hydrogen atom remain attach only to other aluminum atom.

Li₂Al₂H₃ and Li₂Al₂H₄. The geometry optimization for

TABLE I. The comparison of calculated and experimental binding energy and bond lengths of all homoatomic and heteroatomic dimers studied in this work. ΔE and ΔR represent the difference between calculated and available experimental values in binding energies and bond lengths, respectively. Experimental values are from Ref. 16.

Dimer	Method	Bond strength (eV)	Exp. value	ΔE	Bond length (Å)	Exp. value	ΔR
H-H							
	DFT (Ref. 13)/6-311++G(d,p)						
	VWN (Ref. 13)	5.00	4.52	-0.48	0.72	0.74	0.02
	BHHLYP (Ref. 13)	4.69	4.52	-0.17	0.74	0.74	0
	PBELYP (Ref. 17)	4.70	4.52	-0.18	0.75	0.74	-0.01
	BLYP (Ref. 13)	4.73	4.52	-0.21	0.75	0.74	-0.01
	B3LYP (Ref. 13)	4.76	4.52	-0.24	0.74	0.74	0
	MP2 (Ref. 14)						
	6-31G(d,p)	4.38	4.52	0.14	0.73	0.74	0.01
	6-311++G(d,p)	4.37	4.52	0.15	0.74	0.74	0
	cc-pVTZ(core=0)	4.49	4.52	0.03	0.74	0.74	0
Li-H							
	DFT/6-311++G(d,p)						
	VWN	2.69	2.47	-0.22	1.57	1.59	0.02
	BHHLYP	2.45	2.47	0.02	1.59	1.59	0
	PBELYP	2.53	2.47	-0.06	1.6	1.59	-0.01
	BLYP	2.50	2.47	-0.03	1.6	1.59	-0.01
	B3LYP	2.52	2.47	-0.05	1.59	1.59	0
	MP2						
	6-31G(d,p)	1.96	2.47	0.51	1.62	1.59	-0.03
	6-311++G(d,p)	2.11	2.47	0.36	1.6	1.59	-0.01
	cc-pVTZ(core=0)	2.24	2.47	0.23	1.59	1.59	0
Al-H							
	DFT/6-311++G(d,p)						
	VWN	3.30	2.95	-0.35	1.62	1.65	0.03
	BHHLYP	3.09	2.95	-0.14	1.65	1.65	0
	PBELYP	3.11	2.95	-0.16	1.68	1.65	-0.03
	BLYP	3.09	2.95	-0.14	1.68	1.65	-0.03
	B3LYP	3.12	2.95	-0.17	1.66	1.65	-0.01
	MP2						
	6-31G(d,p)	2.79	2.95	0.16	1.65	1.65	0
	6-311++G(d,p)	2.87	2.95	0.08	1.64	1.65	0.01
	cc-pVTZ(core=0)	2.95	2.95	0	1.65	1.65	0
Al-Al							
	DFT/6-311++G(d,p)						
	VWN	0.54	1.38	0.84	2.47	2.47	0
	BHHLYP	0.93	1.38	0.45	2.5	2.47	-0.03
	PBELYP	1.34	1.38	0.04	2.53	2.47	-0.06
	BLYP	1.27	1.38	0.11	2.53	2.47	-0.06
	B3LYP	1.17	1.38	0.21	2.51	2.47	-0.04
	MP2						
	6-31G(d,p)	1.12	1.38	0.26	2.48	2.47	-0.01
	6-311++G(d,p)	1.13	1.38	0.25	2.47	2.47	0
	cc-pVTZ(core=0)	1.17	1.38	0.21	2.49	2.47	-0.02

TABLE I. (Continued.)

Dimer	Method	Bond strength (eV)	Exp. value	ΔE	Bond length (Å)	Exp. value	ΔR
Al-Li							
	DFT/6-311++G(d,p)						
	VWN	0.78	0.79	0.01	2.83		
	BHHLYP	0.82	0.79	-0.03	2.87		
	PBELYP	1.03	0.79	-0.24	2.9		
	BLYP	0.94	0.79	-0.15	2.91		
	B3LYP	0.91	0.79	-0.12	2.89		
	MP2						
	6-31G(d,p)	0.65	0.79	0.14	2.89		
	6-311++G(d,p)	0.72	0.79	0.07	2.87		
	cc-pVTZ(core=0)	0.81	0.79	-0.02	2.86		
Li-Li							
	DFT/6-311++G(d,p)						
	VWN	0.93	1.14	0.21	2.7	2.67	-0.03
	BHHLYP	0.88	1.14	0.26	2.7	2.67	-0.03
	PBELYP	1.01	1.14	0.13	2.69	2.67	-0.02
	BLYP	0.89	1.14	0.25	2.71	2.67	-0.04
	B3LYP	0.90	1.14	0.24	2.7	2.67	-0.03
	MP2						
	6-31G(d,p)	0.62	1.14	0.52	2.78	2.67	-0.11
	6-311++G(d,p)	0.73	1.14	0.41	2.75	2.67	-0.08
	cc-pVTZ(core=0)	0.78	1.14	0.36	2.72	2.67	-0.05

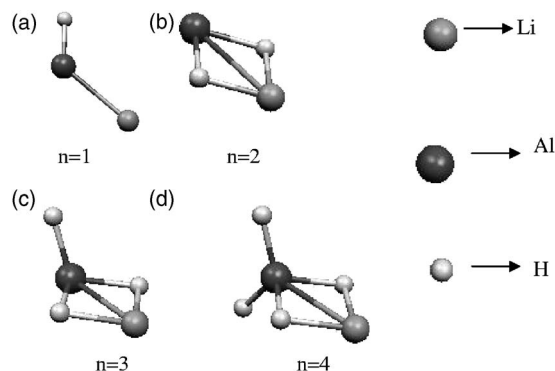
$\text{Li}_2\text{Al}_2\text{H}_3$ and $\text{Li}_2\text{Al}_2\text{H}_4$ clusters was carried out by taking different initial configuration and the ground-state structure along with their higher energy isomer are shown in Figs. 3(h)–3(m). For $\text{Li}_2\text{Al}_2\text{H}_3$ cluster it is seen that the relative orientation of the two hydrogen atoms attached to the different aluminum atoms is significantly changed due to the presence of the third hydrogen atom at the bridge position and the Al-Al distance is also increased slightly as compared to $\text{Li}_2\text{Al}_2\text{H}_2$. In the similar growth motif, the fourth H atom connects at the bridge position of the Al-Al bond from the opposite side of the third H atom and the structure gets more symmetric and therefore the Li_2Al_2 skeleton becomes planar. The bond lengths and energetics of these clusters are shown in Table III. Another isomer [Fig. 3(l)], which is the building

block for higher isomers is 0.05 eV above and has bent Li_2Al_2 structure where each of the aluminum atom is attached to two hydrogen atoms.

$\text{Li}_2\text{Al}_2\text{H}_5$ and $\text{Li}_2\text{Al}_2\text{H}_6$. The ground-state structure for $\text{Li}_2\text{Al}_2\text{H}_5$ cluster was obtained by optimizing the lowest-energy structure of having an extra hydrogen atom attached at different possible locations. The lowest-energy structure for this cluster, the fifth hydrogen atom does not occupy the bridge position between the two aluminum atoms. This is a highly distorted structure where one of the two Al atoms has got three hydrogen atom attached to it and the other Al atom

TABLE II. Interatomic separations (Å) for LiAlH_n clusters.

System	Li-Al	Al-H	Li-H
Li-Al	2.89		
LiAlH	2.66	1.62	
LiAlH ₂	2.68	1.79	1.77
LiAlH ₃	2.58	1.59,1.69	1.80
LiAlH ₄	2.51	1.59,1.69	1.79

FIG. 1. Lowest-energy structures of LiAlH_n ($n=1-4$).

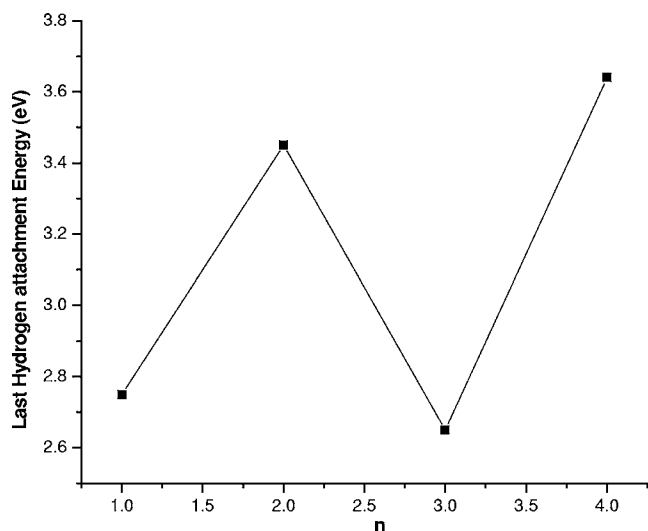


FIG. 2. The hydrogen atom attachment energy [$\Delta E = E(\text{LiAlH}_n) - E(\text{LiAlH}_{n-1}) - E(\text{H})$] on the LiAlH_{n-1} ($n=1-4$) clusters.

has got only two hydrogen atom attached to it. For $\text{Li}_2\text{Al}_2\text{H}_6$ each Al atom is having three hydrogen atoms attached to it and its structure is quite symmetric. The hydrogen atoms in the two AlH_3 units are placed in the eclipsed position. In this context it may be worth to mention that in absence of Li atoms the ground-state geometry of Al_2H_6 shows drastic modifications where two hydrogen atoms (one from each AlH_3 subunit) for bridge site with respect to the two Al atoms.⁸

$\text{Li}_2\text{Al}_2\text{H}_7$ and $\text{Li}_2\text{Al}_2\text{H}_8$. When seventh hydrogen atom is attached to $\text{Li}_2\text{Al}_2\text{H}_6$ cluster the Al-Al bonds get broken as the distance between the two aluminum atom increases to 4.48 Å and the Li_2Al_2 skeleton regains its planarity. Another isomer with Al-Al bond is 0.41 eV higher in energy. The unit also favors the same growth motif as eighth hydrogen. For

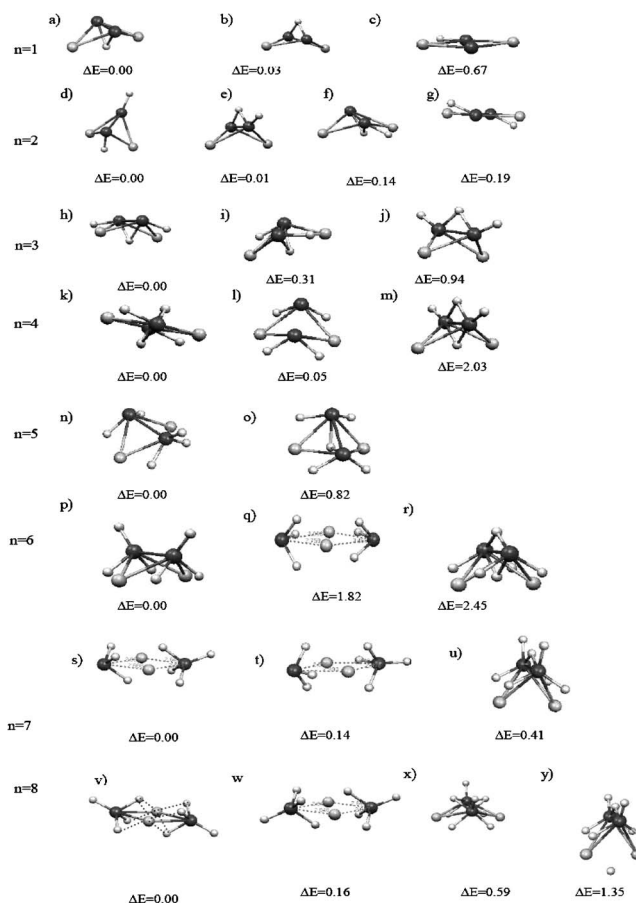


FIG. 3. Geometrical configurations of few low-lying isomers of $\text{Li}_2\text{Al}_2\text{H}_n$ ($n=1-8$) along with the corresponding energy differences of the higher energy isomers with respect to the ground state structure.

$n=8$, the geometry becomes more symmetric as both Al atoms forms ($\text{AlH}_4^{\delta-}$) moiety. This is very similar to what is

TABLE III. The interatomic separations, average binding energy (BE), H—uptake energy and Mulliken point charge distribution of $\text{Li}_2\text{Al}_2\text{H}_n$ clusters obtained at the MP2/cc-pVTZ (PBE-LYP/cc-pVTZ) level. BE ($\text{Li}_2\text{Al}_2\text{H}_n$) = $[E(\text{Li}_2\text{Al}_2\text{H}_n) - 2 \times E(\text{Al}) - 2 \times E(\text{Li}) - n \times E(\text{H})] / n$, H—uptake energy = $[E(\text{Li}_2\text{Al}_2\text{H}_n) - E(\text{Li}_2\text{Al}_2) - n \times E(\text{H})]$.

n	Al-Al (Å)	Al-Li (Å)	Al-H (Å)	Li-H (Å)	BE (eV)	H—uptake energy (eV)	Charge on Al	Charge on Li
0	2.41	2.71			1.19(1.12)		-0.36	0.36
1	2.51	2.71	1.88	2.17	1.51(1.53)	2.80(3.16)	-0.16	0.32
2	2.47	2.62,2.80	1.60,1.76	1.99	1.73(1.76)	5.63(6.09)	0.26, -0.08	0.23
3	2.62	2.59,2.69	1.67,1.79	1.83,2.13	1.87(1.93)	8.29(9.01)	-0.008	0.51
4	2.95	2.53,2.79	1.81,1.83,1.68	1.81,2.11	2.01(2.06)	11.29(11.97)	0.17	0.49
5	2.68	2.68,2.70	1.68,1.59	1.81	2.12(2.16)	14.27(15.00)	0.08,0.51	0.49
6	2.70	2.70	1.69,1.59	1.80	2.25(2.30)	17.78(18.58)	0.47	0.48
7	4.48	2.65,2.67,2.68	1.64,1.58, 1.67,1.68	1.94,2.01	2.25(2.29)	20.02(20.77)	0.34,0.67	0.67
8	4.43	2.65	1.64,1.58,1.68	1.94,2.01	2.37(2.41)	23.69(24.52)	0.57	0.60
9	4.43	2.65	1.64,1.58,1.68	1.94,2.01,2.79	2.19(2.23)	23.71(24.57)	0.57	0.60
10	4.43	2.65	1.64,1.58,1.68	1.94,2.01,2.79	2.36(2.41)	28.20(29.28)	0.57	0.60

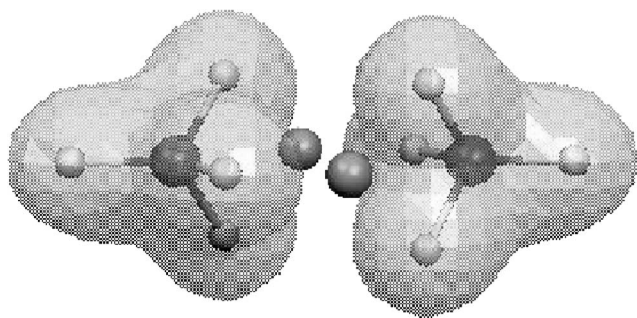


FIG. 4. Isoelectron density (0.02) surface of the $\text{Li}_2\text{Al}_2\text{H}_8$ cluster.

observed in the bulk LiAlH_4 , where four H atoms are tetrahedrally connected to Al forming $(\text{AlH}_4)^{\delta-}$ which is connected to $[\text{Li}]^{\delta+}$ by electrostatic interaction. This aspect is further corroborated by the iso-electron density surface mapping for 0.02 as seen from Fig. 4. We have further noticed that the interatomic distances for Li-H, Al-H of $\text{Li}_2\text{Al}_2\text{H}_n$ reported in Table III, are in very good comparison with the values obtained for bulk material where each Al atom is surrounded by four H atoms having Al-H distances as 1.54 and 1.59 Å and the Li-H separations are between 1.88 and 2.00 Å.¹⁸ It is of significance to note that even the dimer of LiAlH_4 unit shows structural configuration similar to that of bulk LiAlH_4 , where not only do Al atoms have four H atoms for neighbors but also each Li atom is surrounded by four H atoms through weak electrostatic interaction as can be seen from Fig. 3(v). The interatomic separations between Li and four nearby H atoms are in the range of 1.94 and 2.01 Å. This is an important observation where the signature of the structure of bulk material is elegantly reflected in such a small cluster. In order to verify the interaction between two LiAlH_4 units we have calculated the geometry and energetics of different isomers of $\text{Li}_2\text{Al}_2\text{H}_8$ by varying the relative orientation of the two LiAlH_4 units. However, the lowest energy structure was found to be the same as observed from the incremental growth of $\text{Li}_2\text{Al}_2\text{H}_n$ clusters.

$\text{Li}_2\text{Al}_2\text{H}_9$ and $\text{Li}_2\text{Al}_2\text{H}_{10}$. Several atomic configurations were optimized for $n=9$, putting hydrogen at both lithium and aluminum site of $\text{Li}_2\text{Al}_2\text{H}_8$ unit having different orientation. The additional hydrogen atom, if placed inside the cavity of $\text{Li}_2\text{Al}_2\text{H}_8$ unit, was found to fly out spontaneously during relaxation. For $n=10$, two approaches were followed in search of the lowest-energy isomer; in the first case, the

tenth hydrogen atom was placed adjacent to Li and Al atom on $\text{Li}_2\text{Al}_2\text{H}_9$ cluster at various orientation, and in second approach, hydrogen molecule was placed at different possible sites of the $\text{Li}_2\text{Al}_2\text{H}_8$ unit. In particular, when H_2 molecule was put inside the $\text{Li}_2\text{Al}_2\text{H}_8$ cavity, it escapes far apart as shown in Fig. 5. After relaxation, the distances of the atomic and molecular hydrogen from the $\text{Li}_2\text{Al}_2\text{H}_8$ are estimated to be 2.8 and 3.7 Å, respectively. Based on these results it can be infer that the hydrogenation of Li_2Al_2 cluster saturates at $n=8$, which also maintain the bulk composition.

B. Energetic

The stability analysis of the lowest energy isomers of LiAlH_n and $\text{Li}_2\text{Al}_2\text{H}_n$ were evaluated at both DFT and MP2 level of theory using the cc-pVTZ basis set. The results are summarized in Table III. An overall good comparison between the DFT and MP2 results was obtained. The binding energy of $\text{Li}_2\text{Al}_2\text{H}_n$ clusters increases up to $n=8$ and then almost get saturated. For $n=9$, the binding energy of the last hydrogen atom is found to be extremely low indicating that this hydrogen atom is not connected to any atom of the $\text{Li}_2\text{Al}_2\text{H}_8$ unit. For $n=10$, two H atoms form molecular hydrogen and does not bind with $\text{Li}_2\text{Al}_2\text{H}_8$ and thus the average binding energy of $\text{Li}_2\text{Al}_2\text{H}_{10}$ is found to be almost equal to that of $\text{Li}_2\text{Al}_2\text{H}_8$. This fact appears more prominently in the H-uptake energies listed in Table III, where the uptake energy of H atom increases up to $n=8$ and then saturates. For $n=9$, the hydrogen uptake energy remains the same as that of $n=8$. For $\text{Li}_2\text{Al}_2\text{H}_{10}$, the additional uptake energy in comparison to that of $\text{Li}_2\text{Al}_2\text{H}_8$ is basically the molecular binding energy of two H atoms, which is 4.51 eV. Further, to verify the stability of $\text{Li}_2\text{Al}_2\text{H}_8$ cluster we have investigated its interaction with molecular hydrogen. For this purpose the H_2 molecule was placed on top of the tetragonal face and relaxed the geometry. After few steps of ionic iterations the H_2 molecule was found to fly apart of the $\text{Li}_2\text{Al}_2\text{H}_8$, leading to show its inertness to react. Finally the thermo-chemical data of LiAlH_4 and $\text{Li}_2\text{Al}_2\text{H}_8$ clusters have been analyzed based on the heat of formation as obtained by different combinations of reactants. For this purpose both MP2 and DFT results are listed below. (The results obtained at the PBE-LYP/cc-pVTZ level are presented inside parenthesis.) It is seen that MP2 and DFT results are in good agreement. From this list it is clear that both molecular and atomic hydrogen reactions are exothermic on atoms as well as clusters. The very

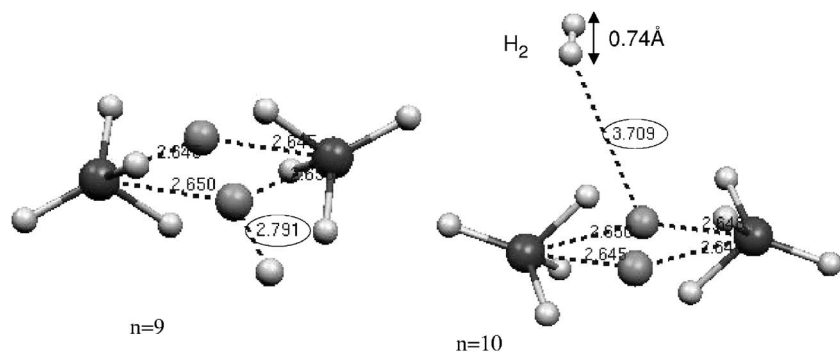
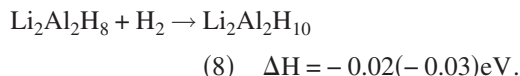
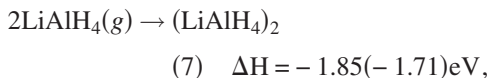
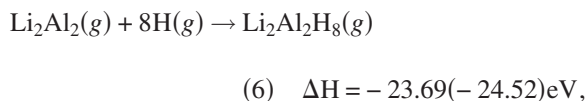
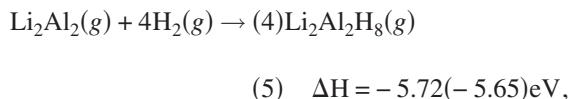
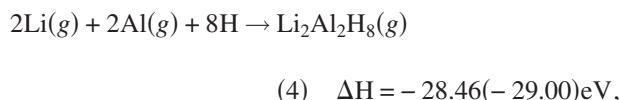
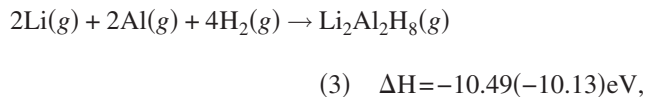
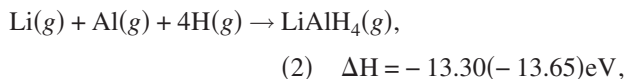
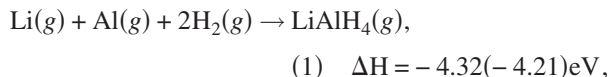


FIG. 5. The lowest-energy isomers of $\text{Li}_2\text{Al}_2\text{H}_n$ ($n=9-10$) clusters.

weak interaction of molecular hydrogen with $\text{Li}_2\text{Al}_2\text{H}_8$ provides evidence for its higher stability.



Another way to show the stability of any species is its inability to donate or accept an electron, which in turn could be assessed from its ionization potential or electron affinity values. Accordingly, the stability of $\text{Li}_2\text{Al}_2\text{H}_8$ was verified by calculating its vertical ionization potential and electron affinity, which are found to be 10.62 and 0.27 eV, respectively. In this context it may be mentioned that for Al_2H_6 , the ionization potential and electronic affinity are reported to be 10.43 and 0.44 eV, respectively.⁸ The close proximity of the IP's and EA's values between these two systems further indicates similar behavior of the highest occupied molecular orbital which is mainly responsible for their electronic properties. The low reactivity and electron affinity coupled with high ionization potential suggest that both LiAlH_4 and $\text{Li}_2\text{Al}_2\text{H}_8$ are highly stable clusters. The values of atomization energy (AE), vertical ionization potentials (VIPs), and vertical electron affinities (VEAs) for LiAlH_4 and $(\text{LiAlH}_4)_2$ clusters are summarized in Table IV. A comparison of the results lead to an important conclusion that the association of two magic clusters can lead to the formation of a significantly more stable dimer, which is unlike the trend shown by normal atomic or molecular clusters. In fact, the monomer LiAlH_4 having eight valence electrons forms a closed shell structure is less stable in comparison to its dimer $(\text{LiAlH}_4)_2$, which has got sixteen valence electrons and does not repre-

TABLE IV. Atomization energy (AE), vertical ionization potentials (VIP), and vertical electron affinities (VEA) for LiAlH_4 and $(\text{LiAlH}_4)_2$ clusters. $\text{AE}(\text{Li}_2\text{Al}_2\text{H}_n) = [E(\text{Li}_2\text{Al}_2\text{H}_n) - 2 \times E(\text{Al}) - 2 \times E(\text{Li}) - n \times E(\text{H})]$, $\text{AE}(\text{LiAlH}_n) = [E(\text{LiAlH}_n) - E(\text{Al}) - E(\text{Li}) - n \times E(\text{H})]$.

System	LiAlH_4	$(\text{LiAlH}_4)_2$
AE(eV)	13.40	28.46
VIP(eV)	10.45	10.62
VEA(eV)	0.38	0.27

sent a closed electron shell. This is a very unusual result. The higher stability of the $(\text{LiAlH}_4)_2$ is attributed to the increased coordination of Li atoms on dimerization. In monomer Li atom is connected to two hydrogen atoms, which is increased to four in the dimer through electrostatic force of attraction between Li and H. This is similar to that of H bonds but opposite in polarity. In our calculation for the dimer, it is found that the Li-H bond energy is 2.24 eV with an interatomic separation of 1.59 Å (Table I) at the MP2/cc-pVTZ level. The large binding energy on dimerization of two stable LiAlH_4 units is a result of increased Li coordination. However, the inter-atomic separation between Li and H atoms in the $\text{Li}_2\text{Al}_2\text{H}_8$ are found to be significantly larger than the free dimer. As a consequence, each Li-H bond would contribute less energy in the $\text{Li}_2\text{Al}_2\text{H}_8$ unit resulting in the gain of total energy 1.85 eV.

IV. CONCLUSION

In conclusion, the hydrogenation behavior of light metals alloy clusters LiAl and $(\text{LiAl})_2$ has been demonstrated by using the post-Hartree-Fock (MP2/cc-pVTZ) and density functional theory under the PBE-LYP exchange correlation functional. The results obtained from both methodologies were found to be in good agreement. Based on the results it is revealed that for LiAl cluster, the saturation composition of hydrogen uptake converges at the monomer itself. Unlike the general trend of small metallic clusters, where the structure and bonding differs considerably to that of bulk, even the dimer of LiAlH_4 unit shows structural configuration similar to that of bulk, where not only Al atoms have four H atoms as its neighbors but also each Li atom is surrounded by four H atom. Most interestingly, it is found that the interaction energy of two LiAlH_4 units is estimated to be 1.85 eV, which is significantly large considering the stability of each monomer unit. Apart from large binding energy, the higher stability of the $\text{Li}_2\text{Al}_2\text{H}_8$ unit is evident from its inertness to react with hydrogen, high ionization potential and low electron affinity than its monomer. This is unlike the trend followed by normal atomic or molecular clusters. The analysis of electronic charge distribution provides evidence for H-bond-like electrostatic interactions with opposite polarity appears when two monomers interact. The higher stability of the dimer in comparison to the monomer unit is attributed to the increased coordination of Li atoms.

ACKNOWLEDGMENTS

We are thankful to the members of the Computer Division, BARC, for their kind cooperation during this work.

*Email address: chimaju@magnum.barc.ernet.in

- ¹W. A. de Heer, *Rev. Mod. Phys.* **65**, 611 (1993); M. Brack, *ibid.* **65**, 677 (1993).
- ²H. Haberland, *Clusters of Atoms and Molecules: Theory, Experiment* (Springer Verlag, New York, 1994).
- ³W. D. Knight, K. Clemenger, W. A. de Heer, W. A. Saunders, M. Y. Chou, and M. L. Cohen, *Phys. Rev. Lett.* **52**, 2141 (1984).
- ⁴D. W. Arnold, S. E. Bradforth, T. N. Kitsopoulos, and D. M. Neumark, *J. Chem. Phys.* **95**, 8753 (1991).
- ⁵S. N. Khanna and P. Jena, *Phys. Rev. Lett.* **69**, 1664 (1992).
- ⁶H. Hakkinen and M. Manninen, *Phys. Rev. Lett.* **76**, 1599 (1996).
- ⁷X. R. Chen, Y. L. Bai, J. Zhu, and X. D. Yang, *Phys. Rev. A* **69**, 034701 (2004).
- ⁸B. K. Rao, P. Jena, S. Burkart, G. Gantefor, and G. Seifert, *Phys. Rev. Lett.* **86**, 692 (2001).
- ⁹J. Chen, N. Kuriyama, Q. Hiroyuki, T. Takeshita, and T. Sakai, *J. Phys. Chem. B* **105**, 11214 (2001); J. Kang, J. Lee, R. P. Muller, and W. A. Goddard III, *J. Chem. Phys.* **121**, 10623 (2004).
- ¹⁰B. K. Rao, S. N. Khanna, and P. Jena, *Phys. Rev. B* **43**, 1416 (1991); *ibid.* **45**, 13 631 (1992); H. Kawamura, V. Kumar, Q. Sun, and Y. Kawazoe, *ibid.* **65**, 045406 (2001); Sergey A. Varganov, Ryan M. Olson, Mark S. Gordon Greg Mills, and Horia Metiu, *J. Chem. Phys.* **120**, 5169 (2004); Young-Kyu Han, Jaehoon Jung, and Kyoung Hoon, *ibid.* **122**, 124319 (2005).
- ¹¹W. Schmidt, K. K. Baldrige, J. A. Boatz, S. T. Elbert, M. S. Gordon, J. H. Jensen, S. Koseki, N. Matsunaga, K. A. Nguyen, J. S. Su, T. L. Windus, M. Dupuis, and J. A. Montgomery, *J. Comput. Chem.* **14**, 1347 (1993).
- ¹²J. B. Foresman and A. Frisch, *Exploring Chemistry with Electronic Structure Methods* (Gaussian, Inc., Pittsburgh, 1995).
- ¹³R. G. Parr and W. Yang, *Density Functional Theory of Atoms Molecules* (Oxford Scientific, Oxford, 1989); S. H. Vosko, L. Wilk, and M. Nusair, *Can. J. Phys.* **58**, 1200 (1980); A. D. Becke, *Phys. Rev. A* **38**, 3098 (1988); A. D. Becke, *J. Chem. Phys.* **98**, 5648 (1993); P. J. Stephens, F. J. Devlin, C. F. Chabrowski, and M. J. Frisch, *J. Phys. Chem.* **98**, 11 623 (1994); R. H. Hertwig and W. Koch, *Chem. Phys. Lett.* **268**, 345 (1997).
- ¹⁴M. Haser, J. Almlof, and G. E. Scuseria, *Chem. Phys. Lett.* **181**, 497 (1991); C. Moller and M. S. Plesset, *Phys. Rev.* **46**, 618 (1934); W. J. Hehre, L. Radom, V. P. R. Schleyer, and J. A. Pople, *Ab Initio Molecular Orbital Theory* (Wiley, New York, 1985).
- ¹⁵H. Dunning, Jr., *J. Chem. Phys.* **90**, 1007 (1989); D. E. Woon and T. H. Dunning, Jr., *ibid.* **98**, 1358 (1993); R. Krishnan, J. S. Binkley, R. Seeger, and J. A. Pople, *ibid.* **72**, 650 (1980); A. D. McLean and G. S. Chandler, *ibid.* **72**, 5639 (1980); R. Ditchfield, W. J. Hehre, and J. A. Pople, *ibid.* **54**, 724 (1971); W. J. Hehre, R. Ditchfield, and J. A. Pople, *ibid.* **56**, 2257 (1972); J. D. Dill and J. A. Pople, *ibid.* **62**, 2921 (1975); M. M. Francl, W. J. Pietro, W. J. Hehre, J. S. Binkley, M. S. Gordon, D. J. DeFrees, and J. A. Pople, *ibid.* **77**, 3654 (1982).
- ¹⁶*CRC Handbook of Chemistry and Physics*, 49th ed., edited by R. C. Weast (CRC Press, Cleveland, Ohio, 1969).
- ¹⁷J. P. Perdew, K. Burke, and M. Ernzerhof, *Phys. Rev. Lett.* **77**, 3865 (1996); **78**, 1396(E) (1997); M. Ernzerhof and G. E. Scuseria, *J. Chem. Phys.* **110**, 5029 (1999); C. Lee, W. Yang, and R. G. Parr, *Phys. Rev. B* **37**, 785 (1988).
- ¹⁸N. Sklar and Ben Post, *Inorg. Chem.* **6** 669 (1967); B. C. Hauback, H. W. Brinks, and H. Fjellvag, *J. Alloys Compd.* **346**, 184 (2002).